PROTEINS: Structure, Function, and Genetics 37:729–742 (1999)

Insights Into the Mechanisms of Catalysis and Heterotropic Regulation of *Escherichia coli* Aspartate Transcarbamoylase Based Upon a Structure of the Enzyme Complexed With the Bisubstrate Analogue *N*-phosphonacetyl-L-aspartate at 2.1 Å

Lei Jin,[1] Boguslaw Stec,[2] William N. Lipscomb,[3] and Evan R. Kantrowitz[1]*
[1]*Department of Chemistry, Boston College, Merkert Chemistry Center, Chestnut Hill, Massachusetts*
[2]*Department of Biochemistry and Cell Biology, Rice University, Houston, Texas*
[3]*Department of Chemistry, Harvard University, Gibbs Laboratory, Cambridge, Massachusetts*

ABSTRACT **A high-resolution structure of *Escherichia coli* aspartate transcarbamoylase has been determined to 2.1 Å; resolution in the presence of the bisubstrate analog *N*-phosphonacetyl-L-aspartate (PALA). The structure was refined to a free R-factor of 23.4% and a working R-factor of 20.3%. The PALA molecule is completely saturated with interactions to side chain and backbone groups in the active site, including two interactions that are contributed from the 80s loop of the adjacent catalytic chain. The charge neutralization of the bound PALA molecule (and presumably the substrates as well) induced by the electrostatic field of the highly positively charged active site is an important factor in the high binding affinity of PALA and must be important for catalysis. The higher-resolution structure reported here departs in a number of ways from the previously determined structure at lower resolution. These modifications include alterations in the backbone conformation of the C-terminal of the catalytic chains, the N- and C-termini of the regulatory chains, and two loops of the regulatory chain. The high-resolution of this structure has allowed a more detailed description of the binding of PALA to the active site of the enzyme and has allowed a detailed model of the tetrahedral intermediate to be constructed. This model becomes the basis of a description of the catalytic mechanism of the transcarbamoylase reaction. The R-structural state of the enzyme-PALA complex is an excellent representation of the form of the enzyme that occurs at the moment in the catalytic cycle when the tetrahedral intermediate is formed. Finally, improved electron density in the N-terminal region of the regulatory chain (residues 1 to 7) has allowed tracing of the entire regulatory chain. The N-terminal segments of the R1 and R6 chains are located in close proximity to each other and to the regulatory site. This portion of the molecule may be involved in the observed asymmetry between the regulatory binding sites as well as in the heterotropic response of the enzyme. Protein 1999;37: 729–742.** © **1999 Wiley-Liss, Inc.**

Key words: allosteric regulatory; enzyme-inhibitor complex; cooperativity; tetrahedral intermediate

INTRODUCTION

Aspartate transcarbamoylase (E.C.2.1.3.2) catalyzes the formation of *N*-carbamoyl-L-aspartate and inorganic phosphate from carbamoyl phosphate and L-aspartate. In many prokaryotes such as *Escherichia coli* this reaction is the committed step in pyrimidine biosynthesis. To regulate the entire pyrimidine pathway, the activity of aspartate transcarbamoylase is regulated by the relative concentration of its substrate aspartate (homotropic effect) and the end products of both the pyrimidine and purine biosynthesis pathways (heterotropic effect).[1] Cytidine 5′-triphosphate (CTP) and uridine 5-triphosphate (UTP), the end products of pyrimidine biosynthesis, inhibit the enzyme;[1] however, UTP only inhibits the enzyme in the presence of CTP.[2] Adenosine 5-triphosphate (ATP), the end product of the parallel purine biosynthesis pathway, activates the enzyme.[1] The opposing regulation by the purine and pyrimidine nucleotides provides the cell a mechanism for balancing the levels of these nucleotides for nucleic acid biosynthesis.

In eukaryotes, aspartate transcarbamoylase is often found in a multienzyme complex covalently associated with one or more enzymes involved in pyrimidine biosyn-

Abbreviations: PALA, *N*-phosphonacetyl-L-aspartate; CP, carbamoyl phosphate; Al, allosteric; rms, root mean square; PDB, Brookhaven Protein Data Bank; 8atc, the R-state structure of aspartate transcarbamoylase with PALA bound deposited in the Protein Data Bank determined to 2.5 Å; resolution; 6at1, the T-state structure of aspartate transcarbamoylase deposited in the Protein Data Bank determined to 2.6 Å; resolution.

Grant sponsor: National Institutes of Health; Grant numbers GM 26237 and GM06920.
*Correspondence to: Evan R. Kantrowitz, Department of Chemistry, Merkert Chemistry Center, Boston College, Chestnut Hill, MA 02467. E-mail: evan.kantrowitz@bc.edu
Received 27 April 1999; Accepted 6 July 1999

thesis.[3,4] A common feature of all aspartate transcarbamoylases is that they are inhibited by *N*-phosphonacetyl-L-aspartate (PALA), an analogue of both natural substrates, carbamoyl phosphate and L-aspartate. PALA combines into one molecule most of the important binding features of both substrates. This compound has been proposed as a transition-state analogue;[5] however, this notion has been questioned because the tetrahedral structure of the expected transition state is not mimicked in this compound.[6] Although other analogues with structures more similar to the proposed transition state of the aspartate transcarbamoylase reaction have been synthesized, no compound has yet been found that inhibits the enzyme better than does PALA, K_i = 27 nM.[5] Because pyrimidine biosynthesis is a requirement for cell division, PALA has been tested as a potential anticancer drug. In fact, Swyryd et al.[7] found that PALA blocked proliferation of mammalian cells in culture, and Tsuboi et al.[8] found that PALA inhibited the growth of colonic cancer cells. These results have led to clinical trials of PALA as an anticancer drug.[9–14]

The aspartate transcarbamoylase from *E. coli* is a dodecamer composed of two catalytic trimers and three regulatory dimers. Both the catalytic and regulatory chains have two structural domains, the aspartate (Asp) and carbamoyl phosphate (CP) domains in the catalytic chain and the allosteric (Al) and zinc (Zn) domains in the regulatory chain.[15] Based upon the structure of the *E. coli* enzyme with PALA bound,[16] determined to 2.5 Å resolution, the binding of PALA induces tertiary conformational changes in both catalytic and regulatory chains. The two domains of the catalytic chain undergo domain closure, whereas the two domains of the regulatory chain undergo domain opening. The binding of PALA also induces a quaternary conformational change involving a rotation and expansion of the molecule by 11 Å along the threefold axis with simultaneous rotations about the three twofold axes, converting the enzyme from the low-activity low-affinity T state to the high-activity high-affinity R state.[16] A modeling study of the low-angle X-ray scattering data in solution suggests that the expansion and rotations are even larger than those observed in the crystal.[17]

Here we report a significantly higher resolution structure of *E. coli* aspartate transcarbamoylase with PALA bound. The high resolution of this structure has allowed a more detailed description of the binding of PALA to the active site of the enzyme and has allowed a detailed model of the tetrahedral intermediate to be constructed. This model becomes the basis of a description of the catalytic mechanism of the transcarbamoylase reaction. In addition, sufficient electron density was observed to trace the N-terminal of the regulatory chains, which was not observed in the previous structure.[16] This N-terminal loop, which is in close proximity to the regulatory binding site, may play a role in the regulatory properties of the enzyme.

MATERIALS AND METHODS

Materials

Q-Sepharose Fast Flow resin was purchased from Pharmacia. Tris, ampicillin, potassium dihydrogen phosphate, 2-mercaptoethanol, sodium EDTA, sodium azide, and uracil were purchased from Sigma Chemical Company. Agarose, electrophoresis-grade acrylamide, and enzyme-grade ammonium sulfate were purchased from ICN Biomedicals. Casamino acids, yeast extract, and tryptone were obtained from Difco. PALA was a gift of the National Cancer Institute.

Methods

Enzyme purification and concentration determination

The holoenzyme of *E. coli* aspartate transcarbamoylase was isolated as described by Nowlan and Kantrowitz[18] from *E. coli* strain EK1104 containing the plasmid pEK2.[18] The concentration of pure holoenzyme was determined by absorbance measurements at 280 nm with an extinction coefficient of 0.59 cm^2/mg.[19]

Crystallization and data collection

The enzyme was crystallized in the presence of PALA by microdialysis[20] using the previously reported conditions.[21] The crystals, which were hexagonal rods, appeared after approximately 1 week in a microdialysis chamber where the enzyme concentration was 18 mg/mL, and the buffer pH was 5.9. Crystals were mounted in glass capillaries before data collection.

The data were collected at the Crystallographic Facility in the Chemistry Department of Boston College with Cu K radiation on the Area Detector Systems MARK II system mounted on Rigaku RU-200 rotating anode generator operated at 50 kV and 150 mA. A DEC-Alpha 3300 computer controlled the data collection. Diffraction data were collected to 2.1 Å with R_{merge} = 7.0%. Of the unique reflections possible at 2.1 Å resolution, 94% were collected with an average redundancy of 3.8. The reflections after correction were scaled and merged by using the software provided by Area Detector Systems.

The space group (P321) was the same as reported previously,[21] and the unit cell dimensions ($a = b$ = 122.24 Å, c = 156.36 Å) were similar to those reported previously ($a = b$ = 122.11 Å, c = 156.17 Å). The asymmetric unit of the crystal is composed of two catalytic and two regulatory chains, which are labeled C1, C6, R1, and R6, respectively. The remainder of the molecule can be generated by rotations about the threefold axis.

Structure refinement

The initial model used for the structure refinement was an unpublished structure of a mutant version of aspartate transcarbamoylase (Asp-162→Ala) with PALA bound, which was derived from the Brookhaven Protein Data Bank (PDB) file 8atc[16] and refined in our laboratory. The alanine side chain at position 162 was replaced with aspartate using the program O.[22] The entire process of refinement utilized IMPLOR (PolyVision, Inc. Hopedale, MA), a Korn shell script that automates the XPLOR[23] refinement steps. The system works by setting the desired number of test sets (in our case four) to monitor R_{free} at all stages of the refinement. One data set was used for one particular step to avoid overfitting, and the step is ac-

cepted only if the R_{free}decreases and the difference of $R - R_{free}$ does not increase.

At each stage of the refinement, water molecules were automatically added using IMPLOR at positions indicated by their density in omit maps (F_o-F_c). New water molecule positions are accepted only if they are within reasonable hydrogen bonding distance with other atoms in the model. After each cycle of refinement, coordinates of the water molecules with temperature factors greater than 79.9 Å^2 were deleted from the model and checked against the omit density after the next refinement cycle. At the end of the refinement 617 water molecules had been added to the structure (926 amino acids).

The refinements was carried out using the Silicon Graphics Indigo II computers at Boston College. The refined model was visualized and modified against $2F_o$-F_c and F_o-F_c maps using O. The stereochemical properties of the intermediate and the final structures were checked by PROCHECK.[24] Refinement was considered complete when each of the available procedures, including the water building, failed to reduce further the R_{free}. The final refinement statistics are summarized in Table I. The coordinates from the final refinement have been deposited in the PDB.

Structure comparisons

The method for comparing this structure with other deposited T (PDB code 6at1) and R (PDB code 8atc) structures of aspartate transcarbamoylase is a modification of the method described by Williams et al.[25] Only the α-carbon atom coordinates of the α-helices and β-strands of the regulatory and catalytic chains were used for superposition and calculation of root mean square (rms) deviations and planar angles. The loop and turn regions were excluded because of their flexible nature and significant positional variations in different structures. The α-carbon atom coordinates selected were 5c-32c,[†] 37c-74c, 87c-140c, and 292c-305c for the carbamoyl phosphate domain; 141c-231c, 248c-269c, and 273c-291c for the aspartate domain; 15r-48r and 56r-100r for the allosteric domain; and 101r-128r and 134r-149r for the zinc domain. The geometric center for each domain was calculated by adding the x, y, and z coordinates of all the selected α-carbon atoms, respectively, and then obtaining the averaged x, y, and z coordinates. The hinges between domains were chosen carefully by examining the structure using O. The hinges chosen were the α-carbon atom of 140c between the CP and Asp domains, 115r between the CP and zinc domains, 100r between the allosteric and zinc domains, and the average coordinate of the two 44r α-carbon atoms from the R1 and R6 chains between the allosteric domains of R1 and R6.

Superposition of structures and subsequent calculations of the rms deviations as well as calculations of the planar angles were performed in QUANTA (Biosym/MSI). For the planar angle calculation, the coordinates of the geographic centers of the domains and the hinges were input into QUANTA. The planar angles are as defined by Williams et al.[25] The planar angle X is the angle between two centers of gravity and the hinge between the two domains in the same molecule. When one of the domains in two structures was superimposed, the Y angle was defined as the angle

[†]A "c" or "r" is appended to the residue number to indicate the catalytic or regulatory chain, respectively.

TABLE I. Data Collection and Refinement Summary of the Aspartate Transcarbamoylase With PALA Bound

Data collection				
Space group			P321	
d_{min} (Å)			2.1	
Unique reflections			74,685	
Redundancy			3.8	
Completeness (%)			94	
Unit cell[a] (Å)			$a = b = 122.24$	
			$c = 156.36$	
Final R_{merge}[b] (%)			7.0	
Refinement				
Resolution range (Å)			8–2.1	
Sigma cutoff (σ)			2	
Reflections			73,113	
Non-hydrogen protein atoms			7,418	
Water molecules			617	
Working R-factor				
Beginning			31.3	
End			20.3	
Free R-factor				
Beginning			31.3	
End			23.4	
Average B factors (main chain/side chain)				
C1			25.1/27.1	
R1			52.6/56.1	
C6			20.3/22.7	
R6			54.3/56.4	
Refinement (highest resolution shell)				
Resolution range (Å)			~2.2–2.1	
Completeness (%)			91	
R_{merge}[b] (%)			43	
Working R-factor			34.0	
Free R-factor			36.4	
Statistics (rms deviations)				
Bonds (Å)			0.015	
Angles (degrees)			1.74	
Dihedrals (degrees)			25.35	
Impropers (degrees)			1.74	
Average B factors for each domain				
Chain	C1		C6	
Domain	CP	Asp	CP	Asp
B-factor	21.9	30.2	19.1	23.9
Chain	R1		R6	
Domain	Al	Zn	Al	Zn
B-factor	62.4	39.1	63.9	39.1

[a]Unit cell dimensions of the 8atc structure: $a = b = 122.11$, $c = 156.17$.

[b] $R_{merge} = \dfrac{\sum_{hkl}\sum_{i}|I_{mean} - I_i|}{\sum_{hkl}\sum_{i} I_i}$

Al, allosteric; Asp, aspartate; CP, carbamoyl phosphate; Zn, zinc.

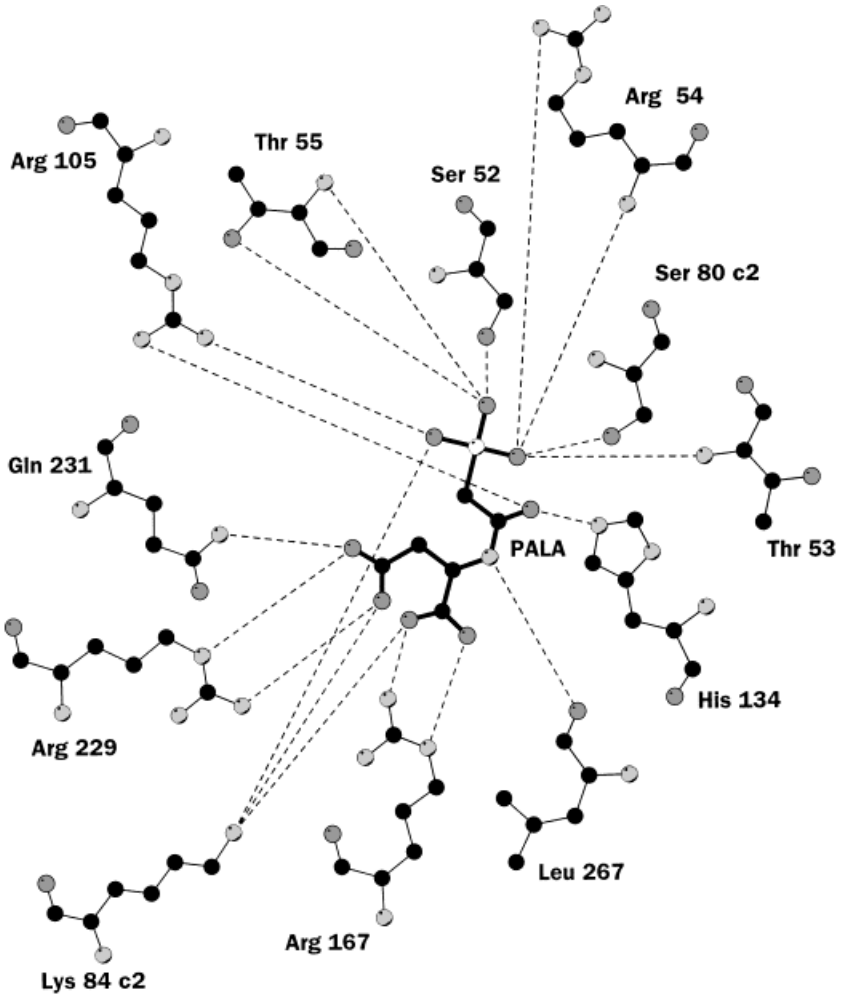

Fig. 1. Schematic diagram of the PALA binding site in the C1 chain of aspartate transcarbamoylase. Shown are all of the residues that have hydrogen bonding interactions (dashed lines) with PALA. The only substantial difference between the C1 and C6 active sites is a reorientation of the side chain of Arg54. This figure was drawn with the program LIGPLOT.[45]

between the centers of gravity of the same comparing domain of the two structures at the average coordinate of the common hinge.

RESULTS

PALA Binding Site

The active sites of aspartate transcarbamoylase are at the interfaces between two adjacent catalytic chains. Furthermore, as has been demonstrated by biochemical studies,[26] residues from both chains are required for enzymatic activity. Residues that interact with PALA include Ser52, Thr53, Arg54, Thr55, Arg105, His134, Arg167, Arg229, Gln231, and Leu267 (backbone) along with Ser80 and Lys84 from the adjacent catalytic chain. Shown in Fig. 1 are the interactions between these residues and the PALA molecule in the C1 active site. The interactions are essentially identical in the C6 active site except for a reorientation of the guanidinium group of Arg54. Noteworthy is the number of interactions to the PALA molecule and the number of these that involve positively charged amino acid side chains (see Table II). Clearly, the electrostatic neutralization of PALA is extremely important for its binding to the enzyme.

Main Chain Comparison Between the 8atc and the New Structure

Overall, the new structure is very similar to the previously reported structure of the enzyme with PALA bound at 2.5 Å resolution (PDB code 8atc; the 8atc structure). To compare these two structures in more detail, each of the domains in the two independently determined catalytic and regulatory chains (C1:R1 and C6:R6) were superimposed separately between the two structures (Table III). For the superposition the flexible loop regions and termini were omitted in the calculation. The CP, Asp, and Zn domains are very similar, with rms deviations of less than 0.3 Å; however, there are twofold larger deviations in the allosteric domains, with rms deviations of approximately 0.5 Å. The larger rms deviations observed for the allosteric domains can be explained by a mechanical uncoupling from the rest of the molecule, as previously proposed.[27] The major differences of the backbone conformation are located at the C-terminal of the catalytic chain, residue 307 to 310; the N- and C-termini of the regulatory chain, residues 1r to 11r and residues 151r-153r, respectively; as well as two loops of the regulatory chain, the 50s loop,

TABLE II. Interactions with PALA in the Active Site of Aspartate Transcarbamoylase

Residue	Atom	PALA atom[a]	C1 distance[b] (Å)	C6 distance[b] (Å)
Ser52	OG	O3P	2.47	2.46
Thr53	N	O2P	2.88	3.01
Arg54	N	O2P	3.14	2.75
Arg54	NE	O2P	—	3.06
Arg54	NH1	O2P	3.12	—
Arg54	NH2	O2P	—	2.89
Thr55	N	O3P	2.82	2.76
Thr55	OG1	O3P	2.82	2.63
Arg105	NH1	O1	2.64	2.98
Arg105	NH2	O1P	2.63	3.35
His134	NE2	O1	2.57	2.90
Arg167	NE	O2	2.73	2.75
Arg167	NH2	O3	2.97	3.16
Arg229	NE	O5	2.71	2.86
Arg229	NH2	O4	2.87	2.94
Gln231	NE2	O5	3.12	—
Leu267	O	N2	3.06	2.93
Ser80[c]	OG	O1P	3.30	2.97
Ser80[c]	OG	O2P	2.77	3.16
Lys84[c]	NZ	O3	3.02	2.91
Lys84[c]	NZ	O4	2.67	2.99
Lys84[c]	NZ	O1P	2.90	2.77

[a]The notations used for the atoms in the PALA molecule are as follows:

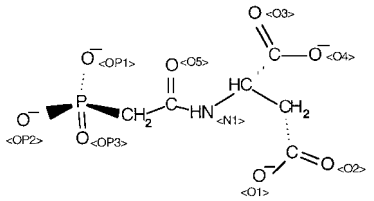

[b]C1 and C6 refer to the two independent catalytic chains in the asymmetric unit.
[c]Ser80 and Lys84 are contributed into the active site from the adjacent catalytic chain.

TABLE III. Comparison of Domains Between This Structure and 8atc When the Carbamoyl Phosphate Domains of C1 are Aligned[†]

Chain[a]	Domain	rms deviation (Å)
C1	Aspartate	0.269
R1	Zinc	0.312
R1	Allosteric	0.568
C6	Carbamoyl	0.269
C6	Aspartate	0.275
R6	Zinc	0.291
R6	Allosteric	0.529

[†]The rms deviation of the C1 CP domains in the two structures was 0.201 Å.
[a]The chain designations used for 8atc are different from all other deposited aspartate transcarbamoylase coordinates. For these comparisons, C1 was compared with the 8atc chain labeled C, R1 with the 8atc chain labeled D, C6 with the 8atc chain labeled A, and R6 with the 8atc chain labeled B.

residues 48r to 55r, in the allosteric domain and the 130s loop, residues 129r to 133r, in the zinc domain.

Regulatory Chain 50s and 130s Loops

When the new and 8atc structures are compared, two loop regions, the 50s and 130s loops, of the regulatory chain exhibit differences corresponding to slightly different conformations. The altered conformation of the 50s loop does result in significant reorientations of the side chains of Glu52r and Met53r. This altered conformation may reflect different conformational substates present upon binding of the regulatory effectors. The conformational change at the end of the loop would influence Lys56r, which has been directly implicated in altering the binding affinities of the regulatory effectors.[28]

Interfaces Between the Chains

Critical for the function of aspartate transcarbamoylase are the interactions between the catalytic and regulatory chains of the enzyme.[29] During the conversion of the enzyme from the T to the R state, numerous interactions that stabilize the T state are broken while numerous other interactions that stabilize the R state are formed. Critical for stabilization of the T state of the enzyme are interactions between the 240s loop of one catalytic chain (C1) to either a catalytic chain (C4) or a regulatory chain (R4) in the opposite half of the molecule, C1-C4 and C1-R4 interactions. In the new structure of the enzyme with PALA bound reported here, no polar C1-C4 or C1-R4 interactions are observed (see Table IV). The polar interactions between the adjacent catalytic chains (C1-C2), regulatory chains of a dimer (R1-R6), and adjacent catalytic and regulatory chains (C1-R1) are provided in Table IV. Noteworthy is the asymmetric nature of the interactions between the catalytic and regulatory chains in the two independent determined interfaces (C1-R1 and C6-R6). Substantially more interactions are observed in the C1-R1 interface than in the C6-R6 interface. These data further support the asymmetric nature of the upper versus lower halves of the enzyme that may be responsible for the observed biphasic binding of the regulatory nucleotides.

Side Chain Conformation Changes

Because of the higher resolution of the new structural data, side chain conformations have been significantly improved in the new structure compared with the 8atc structure. Most of the side chains in the new structure are close to their ideal rotamer positions. A few important side chain corrections were made in the active site of the C1 and C6 catalytic chains (see Fig. 2). The configurations of the guanidinium groups of Arg54 in C6 and Arg229 in both C1 and C6 were reversed, thus allowing them to form ideal and saturated hydrogen bonds to PALA. This is the first time that any asymmetry between configurations of Arg54 in the C1 and C6 chains has been observed.

Geometrical and Conformational Analysis of New, 8atc, and 6at1 Structures

The higher than expected rms deviations for allosteric domains of the regulatory chains (see Table III) may

TABLE IV. Polar Interface Interactions in the New Structure†

C1-R1	C6-R6	C1-C2	R1-R6
Ser11-Glu142	Ser11-Glu142	Glu37-Lys40	Val9*-Val9*
Leu88*-Glu119	Leu88*-Glu119	Gly37-His41	Glu10*-Gln8
Ala89*-Glu119	Ala89*-Glu119	His41*-Arg65	Ala11*-Gln8
Pro107*-Asn113	Pro107*-Asn113	Val43*-Arg65	Thr36*-Gln24
	Gln108-Asn113	Ser52*-Asn78*	Thr38*-Gln24
Gln108-Cys114*	Gln108-Cys114*	Thr53-Ser80	Thr38*-Asn47
Gln109-Asn113	Gln109-Asn113	Arg54-Ser80	Asp39-Arg55
Glu109-Asn111	Glu109-Asn111	Arg54-Glu86	Asp39*-Asn47
	Glu109-Ile115*	Arg54*-Tyr98	Gln40*-Asn47
Glu110*-Tyr140*		Arg56-Gly72*	Arg41-Asn47*
Arg113-Lys139*	Arg113-Lys139	His64-Ser69	Ile42*-Leu46*
	Arg113-Glu142	His64-Val70*	Ile42*-Ile42*
Glu117-Lys139	Glu117-Lys139	Arg65-Tyr98*	Ile44*-Ile44*
Glu117-Tyr140	Glu117-Tyr140	Arg65-Asp100	Leu46*-Ile42*
Ser131-Lys143		Ser74-Asn78	Arg55-Asp39
Asn132-Cys141*	Asn132-Cys141*	Asp75-Asn78	
Asn132-Tyr140*		Asp90-Arg269	
Asn132-Glu142		Thr97-Gly290	
Gln133-Glu142			
Glu196-Arg130			
Tyr197-Lys143			
Asp200-Arg128			
Asp200-Glu144			
Asp200-Arg130			
Glu204-Arg128	Glu204-Arg128		

†All interactions with distances less than 3.8 Å between nitrogen and oxygen are shown. No polar interactions were observed between the C1-R4 and C1-C4 interfaces. Asterisks indicate backbone atoms.

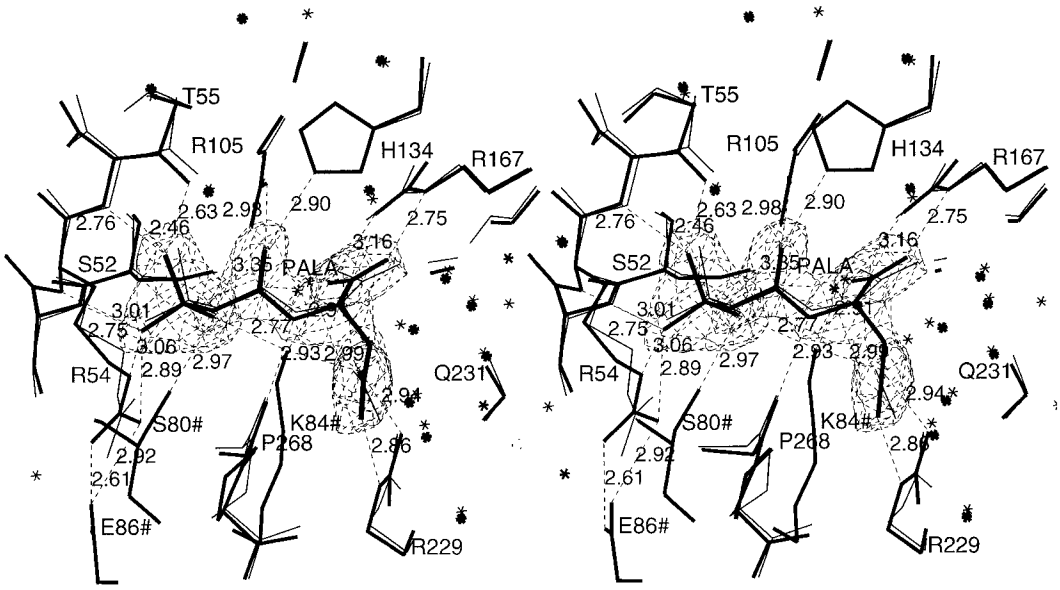

Fig. 2. Stereoview of the C6 active site of aspartate transcarbamoylase with PALA bound. The portion of the 2 F_o-F_c electron density map for PALA is shown (contoured at 2.0 σ) along with a comparison of the side chain conformations of the active site residues in the new (thick lines) and 8atc (thin lines) structures. Water molecules are shown as asterisks. Residue numbers followed by a number sign (#) indicate that these residues are from the adjacent polypeptide chain. Hydrogen bonds are shown as dashed lines.

indicate the existence of the protein in different conformational substates because of a mechanical uncoupling of the allosteric domains from the rest of the molecule.[27] To evaluate the substates more quantitatively we have performed a conformational analysis using the method of Williams et al.[25] This procedure was used to compare the

TABLE V. Comparison of the New PALA-Ligated Structure with the T and R Structures of Aspartate Transcarbamoylase[†]

Domains in comparison[1]	X-planar angles between domains[a] (degrees) 6at1	8atc[b]	New PALA structure
Asp1-CP1	134.11	127.41	127.71
Asp6-CP6	135.69	127.64	128.35
CP1-Zn1	111.17	110.71	111.15
CP6-Zn6	111.26	110.54	110.80
Zn1-Al1	105.56	105.56	104.63
Zn6-Al6	105.62	102.62	103.18
Al1-Al6	153.28	155.52	155.83

[†]The number after the domain name corresponds to the particular chain in the asymmetric unit.
[a]See Materials and Methods for definition of the X-planar angle.
[b]The chain designations used for 8atc are different from all other deposited aspartate transcarbamoylase coordinates. For these comparisons, CP1 and Asp1 were compared with the 8atc chain labeled C, Zn1 and Al1 with the 8atc chain labeled D, CP6 and Asp6 with the 8atc chain labeled A, and Zn6 and Al6 with the 8atc chain labeled B.

new structure of the enzyme with PALA bound to the 8atc and 6at1 structures by calculating the angle and twist among the various domains in the structure. The X-angle represents the degree to which two domains are open whereas the Y-angle represents the relative twist of the two domains. The X-angles between all pairs of domains have been calculated as described in Materials and Methods and are presented in Table V. For both the C1 and C6 chains, the angles between the CP and Asp domains in the new structure are very similar to those in the 8atc structure, but they are smaller than those in the 6at1 structure. The angle between the two allosteric domains of the R1 and R6 chains (Al1-Al6) in the new structure was very similar to that in the 8atc structure, but it was larger than that in the 6at1 structure.

A comparison of the angles between the Zn and Al domains in the R1 and R6 chains of the new structure indicates that they are more symmetric than those of 8atc structure, as opposed to the CP and Asp domains of the catalytic chains, which show a more open and differentiated state (Table V). In the new structure, the angles between CP1 and Zn1 are more open compared with those between CP6 and Zn6 and between Zn1 and Al1 compared with Zn6 and Al6. The angle differences between the CP and Zn domains are smaller than those between the Zn and Al domains.

A comparison of the twist (Y-angle) between the Zn and Al domains in the new and 8atc structures relative to the position of these domains in the 6at1 structure was also performed. Using 6at1, the T-state structure, as a reference, the allosteric domain in the R1 domain of the new structure twisted 0.87 degrees more than it did in the 8atc structure, whereas the R6 allosteric domain of the new structure twisted 0.42 degrees less than it did in the 8atc structure. Furthermore, even between the new and 8atc structures, the R1 and R6 chains exhibited slightly different twist angles (approximately 1°), suggesting that there is a domain motion that cannot be represented by this kind of measurement.

Conformational Change of the 240s Loop in the T→R Transition

Critical for the conversion of the enzyme from the T to the R state is the conformational change of the 240s loop. In the T-state structure, residues of the 240s loop interaction across the C1:C4 and C1:R4 interfaces, forming important T-state stabilizing interactions;[29] however, these interactions are broken during the transition to the R-state when the 240s loop undergoes a significant conformational change. Fig. 3 shows a comparison of the 240s loop in the T and R structures. For this figure we have used the T-state coordinates of the 240s loop from the Thr82r→Ala mutant structure at 2.6 Å (PDB code 1NBE), which was rebuilt during the course of its refinement.[25] The Thr82r→Ala mutation on the regulatory chains of the enzyme should not directly influence the T-state conformation of this loop. When the T- and R-state structures are compared, the alteration in the conformation of the 240s loop results from a very simple rotation of only two peptide bonds (244 and 245), which causes an unwinding of a helical segment between residues 236 and 243 into a more extended conformation. This extended R-state conformation of the 240s loop allows side chains to form intrachain interactions stabilizing the loop's conformation and thereby position side chains to create the high-activity high-affinity active site.

N-termini of the Regulatory Chains

In early structures of aspartate transcarbamoylase, insufficient density was observed for the N-terminal region of the regulatory chains to trace the polypeptide chain, presumably because of the mobility of this area of the structure.[21,30] In the T-state structure of the enzyme with CTP bound, Kosman et al.[31] were able to model the N-terminal of one of the regulatory chains (R1). In the new structure of the enzyme with PALA bound, the electron density associated with the N-terminal region is much weaker than that in other parts of the molecule (compare Fig. 3 and Fig. 4B). However, there was sufficient density to build a tentative model for all the residues. After a number of rebuilding steps, a new model is proposed for the position of the first seven residues along with modifications to the position of residues eight to ten. As seen in Fig. 4, the N-terminal of the R1 chain and that of the R6 chain in the new structure are different from each other, and both are different from the trace determined for the R1 chain in the T-state structure with CTP bound.[31]

C-termini of the Regulatory Chains

Another area of the new structure that is different from the 8atc structure of the enzyme is the C-terminal region of the two regulatory chains. In particular, residues 150r-153r unwind, forming a more extended structure. As seen

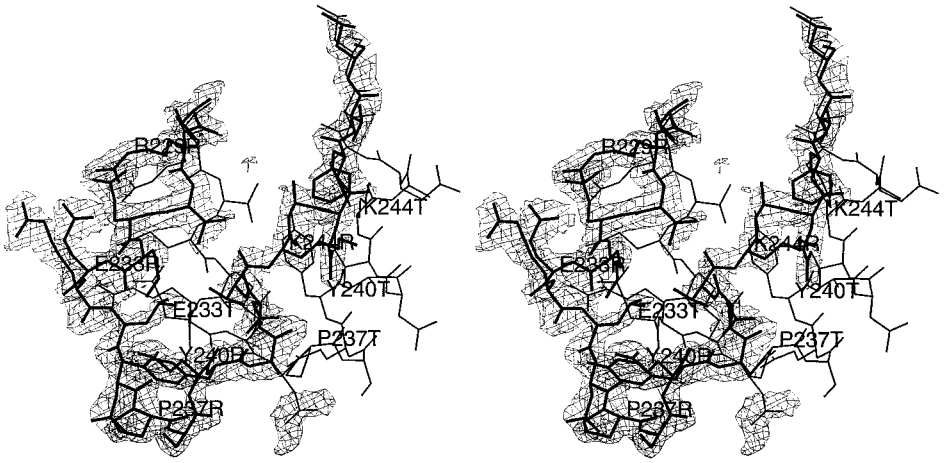

Fig. 3. Stereoview of the 240s loop region. The R-state conformation as determined in the structure reported here is shown with thick lines. The corresponding 240s loop from the T-state structure (Protein Data Bank file 1NBE) is shown with thin lines. The 2 F_o-F_c electron density map of the R-state structure is shown contoured at 1.6 σ.

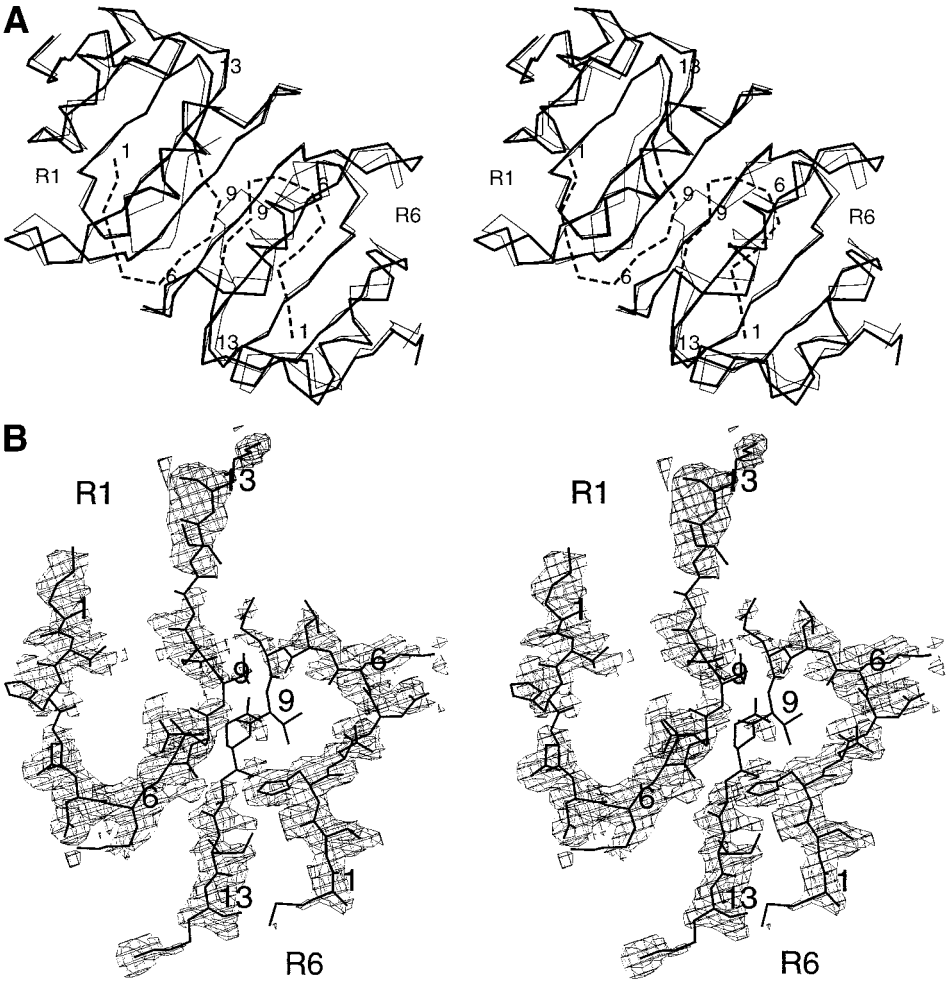

Fig. 4. **A:** A stereoview comparison of the T-state structure (1RAH)[31] (thin lines) and new R-state (heavy lines) structure. Shown is the regulatory dimer composed of the R1 and R6 chains. The newly modeled N-terminal region in the new structure is also shown (heavy broken lines). **B:** Stereoview of the 2 F_o-F_c electron density map for residues 1r to 13r of the R1 and R6 regulatory chains contoured at 1.0 σ. Superimposed upon the electron density is the final model. The orientation of the N-terminal region is identical to that shown in A.

in Fig. 5, the electron density is strong in this region of the structure with only the side chain of Asn153r not completely covered in density. Nevertheless, the trace of the backbone is firmly established and departs from that previously reported. Although the C-terminal of each of the two regulatory chains is slightly different, the overall conformation of the two is similar, and both are different from that in the 8atc structure.

A model of the Proposed Tetrahedral Intermediate

Although PALA binds extremely tightly to aspartate transcarbamoylase and is able to promote the allosteric

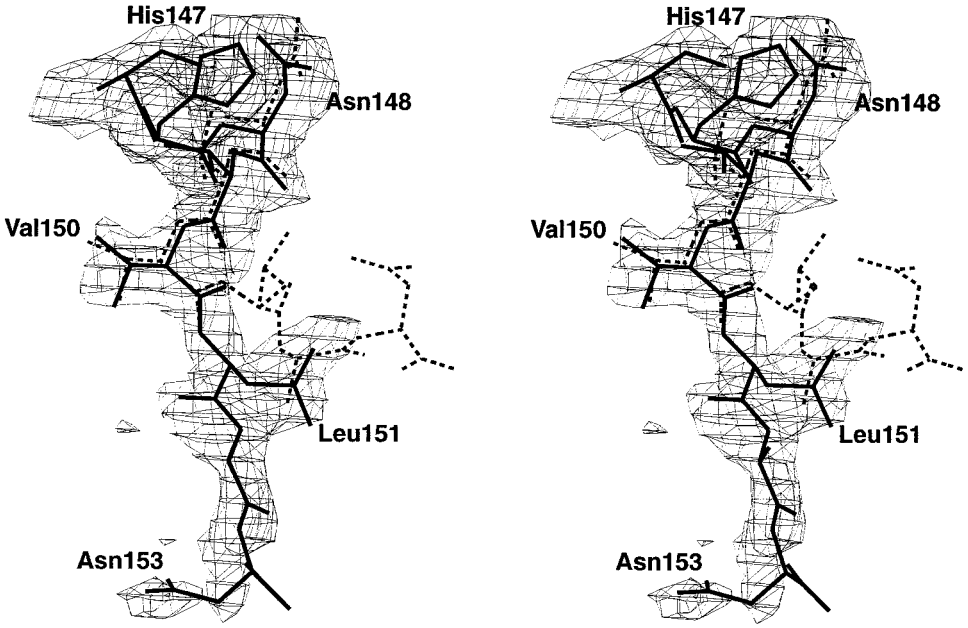

Fig. 5. Stereo view of the electron density map (2 F_o-F_c) for the C-terminal residues (145r to 153r) of the R1 regulatory chain contoured at 1.0 σ. Superimposed upon the electron density is the final refined model (thick lines) as well as the corresponding residues from the 8atc structure (dashed lines). A similar unwinding of the C-terminal is also observed in the R6 chain. This figure was drawn with the program SETOR.[46]

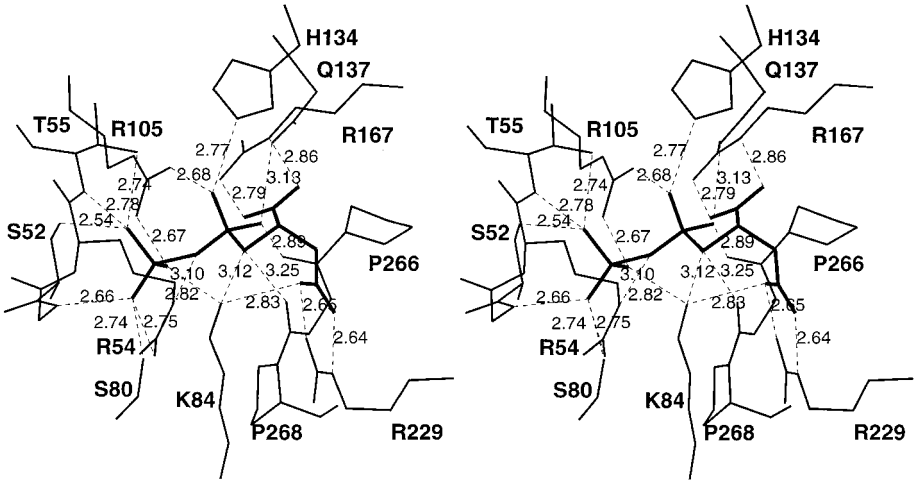

Fig. 6. Stereo view of the C1 catalytic chain of aspartate transcarbamoylase with the tetrahedral intermediate modeled into the active site. Shown are all the side chains that make direct contact with the intermediate from the C1 chain as well as Ser80 and Lys84 from the adjacent catalytic chain. Hydrogen bonds are shown as dashed lines.

transition to the R-structural state, it is not an exact analogue of the transition state because the carbonyl carbon does not have tetrahedral geometry, the amino group of carbamoyl phosphate is lacking, and the ester oxygen between the carbonyl and the phosphorus has been replaced by a methylene bridge. Based upon the structure reported here, we have modeled the proposed tetrahedral intermediate into the active site by replacing PALA and by keeping atoms that are the same in both PALA and the tetrahedral intermediate in similar positions. Necessary minor adjustments were then made to the conformation of the tetrahedral intermediate to optimize interactions. In addition, the conformations of the side chains of Lys84 and Gln137 were altered to improve stereochemistry or contacts. As seen in Fig. 6, the intermediate fits into the position previously occupied by PALA with almost no alteration in the conformation of the protein (see Fig. 2). All the charges of the intermediate are electrostatically neutralized by the protein, and the orientation of the intermediate is positioned with elaborate precision by a variety of hydrogen-bonding interactions.

In this model there are numerous interactions to groups attached to the tetrahedral carbon. For example, the amino group of the intermediate forms interactions with the side chain of Gln137 and the backbone carbonyl of Pro266. The negatively charged oxygen is neutralized by side chain interactions with Arg105 and His134. Furthermore, the ester oxygen interacts with Arg54, and the amide forms hydrogen bonds with Lys84 and the backbone carbonyl of Pro268. The α-carboxylate is neutralized by a bidentate interaction with Arg167, whereas the β-carboxylate is neutralized by interactions with Lys84 and a bidentate interaction with Arg229. Finally, the phosphate is stabilized and neutralized by interactions with Ser52, Thr55, Ser80, Lys84, Arg54, and Arg105.

Our ability to replace the bisubstrate analogue PALA with the structure of the tetrahedral intermediate with almost no alterations in the structure of the enzyme-PALA complex indicates that the structure of the enzyme-PALA complex is an excellent model of the enzyme in its catalytically active conformation.

DISCUSSION

Aspartate transcarbamoylase with PALA bound is considered the R state or high-activity high-affinity state of the enzyme. Given the fact that PALA is also a potential anticancer drug, the structure of the enzyme with PALA bound was reinvestigated, at significantly higher resolution, in the work reported here. The overall quaternary conformational change induced by PALA was similar to that previously reported;[16] however, the new higher-resolution structure provides a significantly improved description of the active site of the enzyme and new details of interactions at the domain interfaces and the N- and C-terminal regions of both the catalytic and the regulatory chains. Those regions were implicated in the homotropic and the heterotropic responses; therefore, the better structural definition will allow us to better understand their function in both catalysis and allosteric control.

Active Site of the Enzyme

As seen in Figs. 1 and 2, the PALA molecule is completely saturated with interactions to side chain and backbone groups in the active site. In fact, every hydrogen bonding donor or acceptor atom on the PALA molecule is involved in at least one interaction. Although most of these interactions come from side chain or backbone residues of the same polypeptide chain that contains the active site, two interactions are contributed from the 80s loop of the adjacent catalytic chain. A comparison of the T- and R-state structures of the enzyme in the vicinity of the active site provides a rationale for the difference in activity and affinity between the T and R states of the enzyme. In the T-state structure, many of the positions of groups interacting with PALA are in alternate conformations, often pointing out of the active site (e.g., Lys84 and Arg229). The free energy associated with the binding of PALA, and presumably the natural substrates as well, induces the closure of the Asp and CP domains, thereby moving critical catalytic groups into their R-state positions (see Fig. 7). In addition, because of steric interference the domain closure requires the associated quaternary conformational change, which also requires a new conformation of the 80s loop, allowing Ser80 and Lys84 to attain their critical conformations that promote catalysis. The charge neutralization of the bound PALA molecule (and presumably substrates as well) induced by the electrostatic field of the highly positively charged active site is an important factor in the high binding affinity of PALA (see Fig. 8).

Implications of the Structure for the Catalytic Mechanism

The high-resolution structure of the complex of aspartate transcarbamoylase and PALA reported here has provided a starting point for the development of a model of the proposed tetrahedral intermediate bound to the active site of enzyme (see Fig. 6), which extends significantly the accuracy attainable in the previous model.[32] These models of the tetrahedral intermediate along with extensive functional data from site-specific mutagenesis allow us to better detail the events that take place during the catalytic cycle of aspartate transcarbamoylase.

As has been well established, the catalytic mechanism for the transcarbamoylase reaction is ordered with carbamoyl phosphate binding before aspartate and *N*-carbamoyl-L-aspartate leaving before phosphate.[33] The enzyme exhibits little affinity for aspartate in the absence of carbamoyl phosphate, and thus the binding of aspartate occurs only to the enzyme–carbamoyl phosphate complex. Evidence from X-ray structural analysis of the enzyme-phosphonoacetamide structure,[34] low-angle X-ray solution scattering,[35] and ultraviolet[36] and circular dichroism[37] spectroscopy indicate that the binding of carbamoyl phosphate induces conformational changes; however, these conformational changes are local and distinct from the large quaternary conformational change that occurs upon aspartate binding. Thus, the binding of carbamoyl phosphate significantly enhances the affinity of the enzyme for aspartate. It is noteworthy that modification of residues involved in carbamoyl phosphate binding such as Thr55, His134, Arg105, and Gln137 has the most dramatic influence on aspartate affinity.[38] Clearly, if carbamoyl phosphate cannot bind or binds in an incorrect orientation, because of alterations in side chain contacts, the binding site of aspartate is not formed correctly.

The mode of PALA binding suggests that Arg105, His134, and Thr55 all interact with the carbonyl oxygen of carbamoyl phosphate thereby enhancing the electrophilicity of the carbonyl carbon for attack by the amino group of aspartate. However, for attack the protonated amino group of aspartate must lose one proton, and a second proton must be lost upon formation of the covalent bond between the amino nitrogen and the carbonyl carbon. The structure of the PALA complex and a model of the proposed tetrahedral intermediate (see Fig. 6) suggest how the protons are removed from the amino group of aspartate. As seen in Fig. 8, the active site pocket is lined with many positively charged side chains forming an extremely electropositive microenvironment. The positive electrostatic field in the active site pocket should lower the pK_a of the amino group of aspartate sufficiently so that the $-NH_3^+$ group loses a proton to solvent as aspartate binds. Two routes are possible for the loss of the next proton from the amino group of aspartate in conjunction with the formation of the tetrahedral intermediate. One possibility, as suggested by Gouaux et al.,[32] is that there is a direct transfer of the proton to the leaving phosphate group. The other possibility is that when the 80s loop of the adjacent catalytic chain swings into the active site, positioning Ser80 and Lys84, the electrostatic environment again is utilized to lower the pK_a of the ϵ-amino group of Lys84, allowing it to act as a base capturing the proton from the amino group of aspartate as the tetrahedral intermediate is formed. In support

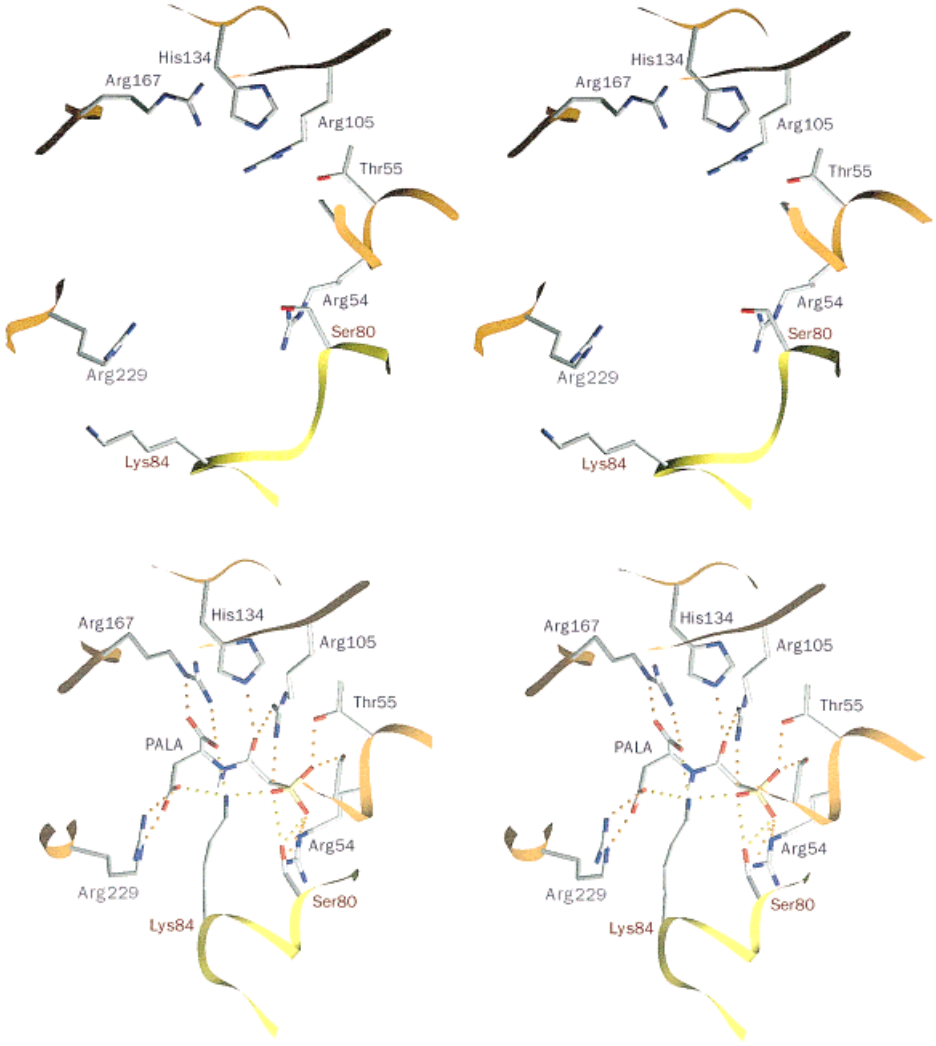

Fig. 7. Stereo view of the active site of aspartate transcarbamoylase in the T (**top panel**) and R (**bottom panel**) active sites. The side chains that interact with PALA in the R state are shown in both panels. The 80s loop of the adjacent catalytic chain, which contributes Ser80 and Lys84 in the active site, is shown in yellow. Note the large number of interactions (dashed lines) with the PALA molecule in the R state (lower panel), many of which are involved in neutralization of the negative charges on the PALA molecule. For clarity Ser52 is not labeled. The data used for the T state of the enzyme (top panel) were from Protein Data Bank file 1NBE. This figure was drawn with the program SETOR.[46]

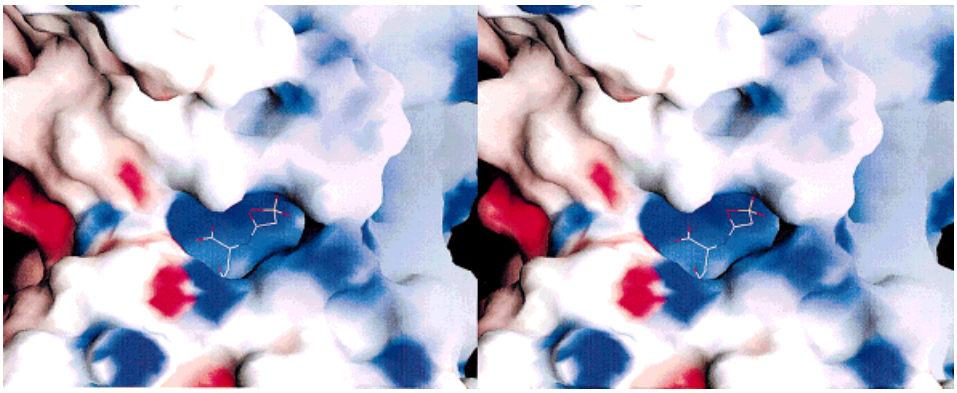

Fig. 8. Stereo view of the C1 catalytic chain of aspartate transcarbamoylase represented as a molecule surface as generated by the program GRASP.[47] Mapped onto the surface is the calculated electrostatic potential. The PALA molecule was placed in the active site after generation of the surface; thus, the blue active site pocket indicates the positive electrostatic potential available to neutralize the highly negatively charged PALA molecule.

of this role for Lys84 is the direct interaction between the ϵ-amino group of Lys84 and the nitrogen of the amino group of aspartate in the tetrahedral intermediate, as well as recent site-specific mutagenesis experiments in which Lys84 was replaced by Asn. The K84N enzyme exhibits more than a 1,200-fold reduction in activity compared with the wild-type enzyme.[39] Upon departure of *N*-carbamoyl-L-aspartate from the active site, the domain-closed conformation, characteristic of the active form of the enzyme, becomes unstable. This results in a possible repositioning of the 80s loop. Because Ser80 and Lys84 both interact with the phosphate-leaving group, this repositioning of the 80s loop may

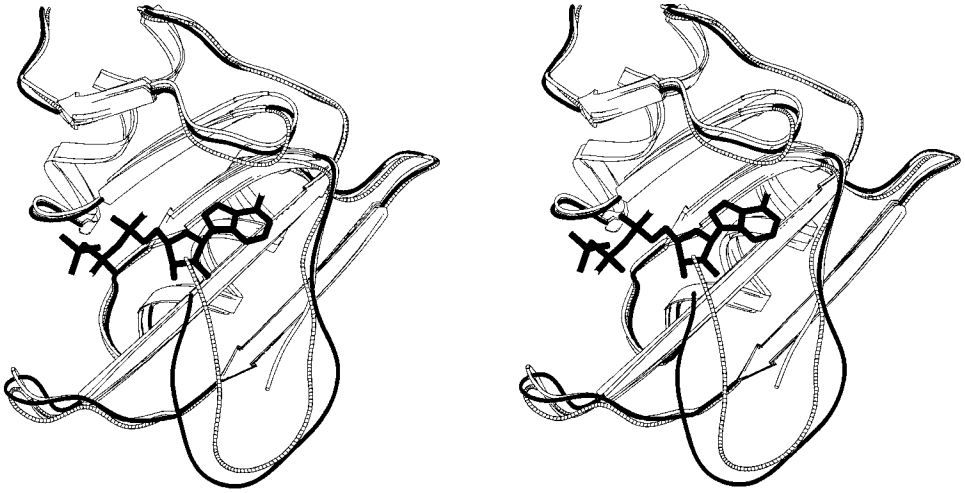

Fig. 9. Stereoview of the allosteric domain of three aspartate transcarbamoylase structures. The open rope corresponds to the R-state structure of the enzyme in the presence of phosphonoacetamide, malonate, and adenosine 5′-triphosphate[48] (PDB code 7at1). In this structure the first seven residues of the regulatory chain could not be resolved because of poor electron density. The striped rope corresponds to the R-state structure of the Thr82→Ala mutant of aspartate transcarbamoylase in the absence of heterotropic effects[25] (PDB code 1NBE). In this structure the entire N-terminal region was fit. Note that the position of the N-terminal residue precludes the binding of the nucleotide. The filled rope corresponds to the R-state structure of the enzyme in the presence of PALA reported here. In the R state, the position of the N-terminal does not preclude the binding of the nucleotide. This figure was drawn with the program SETOR.[46]

provide assistance for the release of phosphate from the highly positively charged active site.

The model of the tetrahedral intermediate also suggests an explanation for the role of Arg54. When Arg54 is replaced by Ala, the activity of the mutant enzyme is reduced by approximately 20,000-fold, with little change in substrate affinity.[40] However, the X-ray structure of the mutant enzyme in the presence of PALA showed that the active site of the enzyme was virtually identical to that of the wild-type enzyme except for the loss of the side chain of Arg54 and the addition of three water molecules in the active site.[41] In the model of the tetrahedral intermediate (see Fig. 6), the side chain of Arg54 interacts with the bridging phosphate oxygen. The neutralization of the developing negative charge on this oxygen as phosphate is expelled would make the phosphate a significantly better leaving group, thereby substantially lowering the activation energy of the reaction. Also observed in the model are some strained hydrogen bonds, which upon phosphate release would straighten, thereby promoting the chemical reaction and the spatial separation of the reaction products.

Conformation of the N-terminal of the Regulatory Chain

In most of the previous structures of aspartate transcarbamoylase, the N-terminal region of the regulatory chains (residues 1r-7r) has not been modeled because of lack of sufficient density in the maps. However, the N-terminal of the R1 chain was modeled in the structure of the enzyme with CTP bound.[31] The location of the N-terminal near the regulatory binding site suggested that it might be involved in the heterotropic interactions of the enzyme. Based upon this structural data, mutagenesis experiments[42,43] were carried out that supported the notion that this region of the regulatory chain is involved in regulation.

In the recently published T-state structure of the unliganded Thr82r→Ala enzyme, a tentative model for the N-terminal fragment of the regulatory chains was proposed,[25] which varied from that reported for the CTP-liganded enzyme.[31] The new model was characterized by placement of the first few residues of the regulatory chain at the nucleotide binding site, and a similar motif is present in the new structure of the PALA-ligated enzyme reported here (see Fig. 9).

In the structure of the enzyme reported here, the electron density in both the R1 and R6 chains was sufficient to model the first seven residues of the N-terminal and to allow a remodeling of residues 8r-10r. As seen in Fig. 9, The new fold, despite being similar to that of the T-state structure, shows some unwinding and opens up the nucleotide binding site more than is observed in the T-state structure.[25] In addition, the trace of the N-terminal residues (1r-7r) was somewhat different in the R1 and R6 chains, suggesting some inherent asymmetry (see Fig. 4). Furthermore, the location of the N-terminal residue itself is extremely close to the nucleotide binding site. Thus, a conformational change in the N-terminal region may be required for the nucleotides to bind. This notion is supported by mutagenesis data that indicate that the binding of CTP is enhanced by approximately fourfold in a mutant enzyme in which the N-terminal of the regulatory chains has been deleted. Furthermore, the observed structural asymmetry of the N-terminal region may be partially responsible for the high- and low-affinity nucleotide binding sites observed by equilibrium dialysis.[44] Thus, the N-terminal region of the regulatory chain is important for

both nucleotide binding and for the heterotropic interactions of aspartate transcarbamoylase.

ACKNOWLEDGMENTS

This work was supported by Grants GM26237 (E.R.K.) and GM06920 (W.N.L.) from the National Institutes of Health.

REFERENCES

1. Gerhart JC, Pardee AB. Enzymology of control by feedback inhibition. J Biol Chem 1962;237:891–896.
2. Wild JR, Loughrey-Chen SJ, Corder TS. In the presence of CTP, UTP becomes an allosteric inhibitor of aspartate transcarbamylase. Proc Natl Acad Sci USA 1989;86:46–50.
3. Coleman PF, Suttle DP, Stark GR. Purification from hamster cells of the multifunctional protein that initiates *de novo* synthesis of pyrimidine nucleotides. J Biol Chem 1977;252:6379–6385.
4. Lue PF, Kaplan JG. Aspartate transcarbamylase and carbamyl phosphate synthetase of yeast: a multifunctional enzyme complex. Biochem Biophys Res Commun 1969;34:426–433.
5. Collins KD, Stark GR. Aspartate transcarbamylase: interaction with the transition state analogue *N*-(phosphonacetyl)-L-aspartate. J Biol Chem 1971;246:6599–6605.
6. Laing N, Chan WWC, Hutchinson DW, Öberg, B. Phosphorus-containing inhibitors of aspartate transcarbamoylase from *Escherichia coli*. FEBS Lett 1990;260:206–208.
7. Swyryd EA, Seaver SS, Stark GR. *N*-(phosphonacetyl)-L-aspartate, a potent transition state analog of aspartate transcarbamylase, blocks proliferation of mammalian cells in culture. J Biol Chem 1974;249:6945–6950.
8. Tsuboi KK, Edmunds HN, Linda K. Selective inhibition of pyrimidine biosynthesis and effect on proliferative growth of colonic cancer cells. Cancer Res 1977;37:3080–3087.
9. Kensler TW, Erlichman C, Jayaram HN, Tyagi AK, Ardalan B, Cooney DA. Peripheral leukocytes as indicators of the enzymic effects of *N*-(phosphonacetyl)-L-aspartic acid (PALA) on human L-aspartate transcarbamoylase (ATCase) activity. Cancer Treat Rep 1980;64:967–973.
10. Madani S, Baillon J, Fries J, et al. Pyrimidine pathway enzymes in human tumors of brain and associated tissues: potentialities for the therapeutic use of *N*-(phosphonacetyl)-L-aspartate and 1-β-D-arabinofuranosylcytsine. Eur J Cancer Clin Oncol 1987;23:1485–1490.
11. Morton RF, Creagan ET, Cullinan SA, et al. Phase II studies of single-agent cimetidine and the combination *N*-phosphonacetyl-L-aspartate (NSC-224131) plus L-alanosine (NSC-153353) in advanced malignant melanoma. J Clin Oncol 1987;5:1078–82.
12. Cohen RE, Schachman HK. Kinetics of the interaction of *N*-(phosphonacetyl)-L-aspartate with the catalytic subunit of aspartate transcarbamoylase. J Biol Chem 1986;261:2623–2631.
13. Ahluwalia GS, Grem JL, Hao Z, Cooney DA. Metabolism and action of amino acid analog anti-cancer agents. Pharmacol Ther 1990;46:243–71.
14. Livingstone LR, White A, Sprouse J, Livanos E, Jacks T, Tisty TD. Altered cell cycle arrest and gene amplication potential accompany loss of wild-type p53. Cell 1992;70:923–935.
15. Honzatko RB, Crawford JL, Monaco HL, et al. Crystal and molecular structures of native and CTP-liganded aspartate carbamoyltransferase from *Escherichia coli*. J Mol Biol 1982;160:219–263.
16. Ke HM, Lipscomb WN, Cho Y, Honzatko RB. Complex of *N*-phosphonacetyl-L-aspartate with aspartate carbamoyltransferase: X-ray refinement, analysis of conformational changes and catalytic and allosteric mechanisms. J Mol Biol 1988;204:725–747.
17. Svergun DI, Barberato C, Koch MHJ, Fetler L, Vachette P. Large differences are observed between the crystal and solution quaternary structures of allosteric aspartate transcarbamylase in the R-state. Proteins 1997;27:110–117.
18. Nowlan SF, Kantrowitz ER. Superproduction and rapid purification of *E. coli* aspartate transcarbamoylase and its catalytic subunit under extreme derepression of the pyrimidine pathway. J Biol Chem 1985;260:14712–14716.
19. Gerhart JC, Holoubek H. The purification of aspartate transcarbamylase of *Escherichia coli* and separation of its protein subunits. J Biol Chem 1967;242:2886–2892.
20. Ke HM, Honzatko RB, Lipscomb WN. Structure of unligated aspartate carbamoyltransferase of *Escherichia coli* at 2.6-Å resolution. Proc Natl Acad Sci USA 1984;81:4027–4040.
21. Krause KL, Voltz KW, Lipscomb WN. 2.5 Å structure of aspartate carbamoyltransferase complexed with the bisubstrate analog *N*-(phosphonacetyl)-L-aspartate. J Mol Biol 1987;193:527–553.
22. Jones TA, Zou JY, Cowan SW, Kjeldgaard M. Improved protein models in electron density maps and the location of errors in these models. Acta Crystallogr 1991;A47:110–119.
23. Brünger AT. X-PLOR, Version 3.1. A system for crystallography and NMR New Haven: Yale University Press; 1992.
24. Laskowski RA, MacArthur MW, Moss DS, Thornton JM. PROCHECK: A program to check the stereochemical quality of protein structures. J Appl Crystallogr 1993;26:283–291.
25. Williams MK, Stec B, Kantrowitz ER. A single mutation in the regulatory chain of *Escherichia coli* aspartate transcarbamoylase is an extreme T-state structure. J Mol Biol 1998;281:121–134.
26. Wente SR, Schachman HK. Shared active sites in oligomeric enzymes: model studies with defective mutants of aspartate transcarbamoylase produced by site-directed mutagenesis. Proc Natl Acad Sci USA 1987;84:31–35.
27. Tanner JJ, Smith PE, Krause KL. Molecular dynamics simulations and rigid body (TLS) analysis of aspartate carbamoyltransferase: evidence for an uncoupled R state. Protein Sci 1993;2:927–935.
28. Corder TS, Wild JR. Discrimination between nucleotide effector responses of aspartate transcarbamoylase due to a singe site substitution in the allosteric binding site. J Biol Chem 1989;264:7425–7430.
29. Kantrowitz ER, Lipscomb WN. *Escherichia coli* aspartate transcarbamoylase: the molecular basis for a concerted allosteric transition. Trends Biochem Sci 1990;15:53–59.
30. Kim KH, Pan Z, Honzatko RB, Ke HM, Lipscomb WN. Structural asymmetry in the CTP-liganded form of aspartate carbamoyltransferase from *Escherichia coli*. J Mol Biol 1987;196:853–875.
31. Kosman RP, Gouaux JE, Lipscomb WN. Crystal structure of CTP-ligated T state aspartate transcarbamoylase at 2.5 Å resolution: implications for aspartate transcarbamoylase mutants and the mechanism of negative cooperativity. Proteins 1993;15:147–176.
32. Gouaux JE, Krause KL, Lipscomb WN. The catalytic mechanism of *Escherichia coli* aspartate carbamoyltransferase: a molecular modeling study. Biochem Biophys Res Commun 1987;142:893–897.
33. Wedler FC, Gasser FJ. Ordered substrate binding and evidence for a thermally induced change in mechanism for *E. coli* aspartate transcarbamylase. Arch Biochem Biophys 1974;163:57–68.
34. Gouaux JE, Lipscomb WN. Crystal structures of phosphonoacetamide ligated T and phosphonoacetamide and malonate ligated R states of aspartate carbamoyltransferase at 2.8 Å resolution and neutral pH. Biochemistry 1990;29:389–402.
35. Fetler L, Tauc P, Vachette P. Carbamyl phosphate modifies the T quaternary structure of aspartate transcarbamylase, thereby facilitating the structural transition associated with cooperativity. J Appl Crystallogr 1997;30:781–786.
36. Collins KD, Stark GR. Aspartate transcarbamylase: studies of the catalytic subunit by ultraviolet difference spectroscopy. J Biol Chem 1969;244:1869–1877.
37. Griffin JH, Rosenbusch JP, Weber KK, Blout ER. Conformational changes in aspartate transcarbamylase. I. Studies of ligand binding and of subunit interactions by circular dichroism spectroscopy. J Biol Chem 1972;247:6482–6490.
38. Stevens RC, Chook YM, Cho CY, Lipscomb WN, Kantrowitz ER. *Escherichia coli* aspartate carbamoyltransferase: the probing of crystal structure analysis via site-specific mutagenesis. Protein Eng 1991;4:391–408.
39. Macol C, Dutta M, Stec B, Kantrowitz ER. The 80s loop of the catalytic chain of *Escherichia coli* aspartate transcarbamoylase is critical for catalysis and homotropic cooperativity. Protein Sci 1999;8:1305–1313.
40. Stebbins JW, Xu W, Kantrowitz ER. Three residues involved in binding and catalysis in the carbamyl phosphate binding site of

Escherichia coli aspartate transcarbamylase. Biochemistry 1989; 28:2592–2600.
41. Stebbins JW, Robertson DE, Roberts MF, Stevens RC, Lipscomb WN, Kantrowitz ER. Arginine 54 in the active site of *Escherichia coli* aspartate transcarbamoylase is critical for catalysis: a site-specific mutagenesis, NMR and X-ray crystallographic study. Protein Sci 1992;1:1435–1446.
42. Dembowski NJ, Kantrowitz ER. The use of alanine scanning mutagenesis to determine the role of the amino terminus of the regulatory chain in the heterotropic mechanism of *Escherichia coli* aspartate transcarbamoylase. Protein Eng 1994;7:673–679.
43. Sakash JB, Kantrowitz ER. The N-terminus of the regulatory chain of *Escherichia coli* aspartate transcarbamoylase is important for nucleotide binding and heterotropic effects. Biochemistry 1998;37:281–288.
44. Winlund CC, Chamberlin MJ. Binding of cytidine triphosphate to aspartate transcarbamylase. Biochem Biophys Res Commun 1970; 40:43–49.
45. Wallace AC, Laskowski RA, Thornton JM. LIGPLOT: a program to generate schematic diagrams of protein-ligand interactions. Prot Eng 1995;8:127–134.
46. Evans SV. SETOR: Hardware-lighted three-dimensional solid representations of macromolecules. J Mol Graph 1993;11:134–138.
47. Nicholls A, Sharp KA, Honig B. Protein folding and association: insights from the interfacial and thermodynamic properties of hydrocarbons. Proteins 1991;11:281–296.
48. Gouaux JE, Stevens RC, Lipscomb WN. Crystal structures of aspartate carbamoyltransferase ligated with phosphonoacetamide, malonate and CTP or ATP at 2.8 Å resolution and neutral pH. Biochemistry 1990;29:7702–7715.